

# Manifold-Based Optimizations for RIS-Aided Massive MIMO Systems

WILSON DE SOUZA JUNIOR<sup>1</sup>, DAVID WILLIAM MARQUES GUERRA<sup>1</sup>, JOSÉ CARLOS MARINELLO<sup>2</sup>, TAUFİK ABRÃO,<sup>1</sup> and EKRAM HOSSAIN<sup>3</sup>

<sup>1</sup>State University of Londrina (UEL), CEP: 86057-970, Londrina, PR, Brazil.

<sup>2</sup>Federal University of Technology - Parana (UTFPR), CEP: 86300-000, Cornélio Procopio, PR, Brazil.

<sup>3</sup>Department of Electrical and Computer Engineering at the University of Manitoba, Winnipeg, Canada.

CORRESPONDING AUTHOR: EKRAM HOSSAIN (e-mail: Ekram.Hossain@umanitoba.ca).

This work was supported in part by the National Council for Scientific and Technological Development (CNPq) of Brazil, Grant: 310681/2019-7, by CAPES, Grant: FC001, in part by Londrina State University (UEL), Brazil, and in part by a Discovery Grant from the Natural Sciences and Engineering Research Council of Canada (NSERC).

**ABSTRACT** Manifold optimization (MO) is a powerful mathematical framework that can be applied to optimize functions over complex geometric structures, which is particularly useful in advanced wireless communication systems, such as reconfigurable intelligent surface (RIS)-aided massive MIMO (mMIMO) and extra-large scale massive MIMO (XL-MIMO) systems. MO provides a structured approach to tackling complex optimization problems. By leveraging the geometric properties of the manifold, more efficient and effective solutions can be found compared to conventional optimization methods. This paper provides a tutorial on MO technique and provides some applications of MO in the context of wireless communications systems. In particular, to corroborate the effectiveness of MO methodology, we explore five application examples in RIS-aided mMIMO system, focusing on fairness, energy efficiency (EE) maximization, intra-cell pilot reuse interference mitigation, and grant-free (GF) random access (RA).

**INDEX TERMS** Manifold Optimization (MO), Reconfigurable Intelligent Surfaces (RIS), Massive MIMO (mMIMO), Energy Efficiency, Grant-free Random Access.

## I. INTRODUCTION

**M**ETHODS based on MO are rooted in their ability to handle complex optimization problems more efficiently and effectively than conventional methods, especially in the context of mMIMO systems, especially for fifth generation (5G) and beyond fifth generation (B5G) communications such as sixth generation (6G) systems.

Many optimization problems in wireless communications involve non-convex constraints, such as those arising from the geometry of the problem space. For instance, in RIS-aided systems, specifically for entirely passive RIS, the imposed phase shifts by the RIS, lie on a unit circle in the complex plane, which forms a non-convex constraint. MO can treat these constraints more naturally by considering the problem as an optimization over a smooth manifold, exploiting *geometric properties* of the problem, and allowing a more efficient solution. This is done by leveraging some ideas, such as the *local linearization*, which is a technique that benefits from the ability to linearize the problem space

locally, e.g., manifolds are locally Euclidean, meaning they can be linearized around any point, allowing the use of linear optimization techniques such as gradient descent and Newton's method in a more generalized form. Another motivation for using manifold-based optimizations is the ability to handle *high-dimensional data*, often present in wireless communication systems, making optimization challenging. For instance, manifold learning techniques can transform high-dimensional data into a more manageable form, improving optimization in signal processing and resource allocation contexts. Finally, MO methods offer versatility to deal with constraints and symmetries, founded in optimization problems that are difficult to handle with traditional optimization methods; for example, MO can handle constraints like *orthonormality*, *low rank*, *positivity*, and even *invariance* under group actions, which are common in wireless communication problems.

TABLE 1: Examples of wireless communication problems solved efficiently by using MO techniques

Wireless example	Problem	MO-based solution
RIS Phase Shift Optimization [1]–[9]	Optimizing the phase shifts of RIS elements to maximize some KPI.	Treating the phase shifts as points on a complex circle manifold allows for more natural and efficient optimization than traditional methods that might struggle with the unit-modulus constraint.
Active beamforming in mMIMO Systems [1], [2]	Optimize the beams to maximize signal strength and minimize interference.	Using MO to represent the beam directions on a particular manifold can lead to better beam selection and alignment performance.
Resource Allocation in B5G Systems [10]	Allocating resources such as power and bandwidth to users in a way that maximizes overall system performance.	Manifold learning techniques can identify clusters of users or resources, simplifying the optimization problem and leading to more efficient allocation strategies.

### A. BACKGROUND

RISs are typically employed to enhance the channel gain between the base station (BS) and the user’s equipment (UE), especially when environmental obstacles blockage direct communication. The passive mode of operation, where the device lacks active radio frequency (RF) components for energy efficiency purposes, is the most desirable scenario for RISs since, in this mode, the RIS does not perform any sophisticated processing on it, reducing its complexity and eliminating eventual overhead in the communication protocol. In this sense, the practical problem of how to configure/optimize the RIS in wireless communications scenarios emerges, imposing some ideas over its potential and physical constraints.

**Wide-beam design (WBD) for RIS-aided systems:** WBD for RIS-aided design refers to the configuration of RIS to create broad, uniform beams that cover larger areas compared to narrow, highly focused beams. This design is crucial when dealing with multi-user (MU), especially in machine massive type communications (mMTC) where many devices are randomly accessing the system. The advantageous features of the WBD for RIS passive beamforming include:

- ◊ *Uniform Coverage*, ensuring that all areas within the specified range receive adequate signal strength, reducing the chances of dead zones.
- ◊ *Simplified Access*: devices can access the network more easily since they do not need to be precisely aligned with a narrow beam.
- ◊ *Reduced Complexity* simplifies the control and management of the beams, as fewer adjustments are needed to maintain coverage.
- ◊ *Support for Mobility*: it better accommodates mobile users as the broad beam can maintain connectivity without frequent reconfiguration.
- ◊ *Improved Access Success Rate*: with uniform, wide-beam coverage, more devices are likely to successfully

access the network on their first attempt, reducing collisions and the need for retransmissions.

- ◊ *Load Balancing*: Wide-beam can distribute the access load more evenly across the coverage area, preventing congestion and improving overall network efficiency.
- ◊ *EE*: devices can transmit at lower power levels as they benefit from the enhanced signal propagation provided by RIS, extending battery life.
- ◊ *Reduced Latency*: By decreasing the probability of access failures and re-transmissions, wide beam design can help reduce access delays, which is critical for time-sensitive internet of things (IoT) applications.

Given the promising gains offered by RISs, their deployment is becoming increasingly essential. However, to achieve the conditions necessary for passive RIS operation, the reflection coefficients must have a unit modulus. This requirement introduces a non-convex constraint, making the optimization process more challenging. To address this, manifold-based algorithms emerge as a promising solution, offering an appealing trade-off between performance and complexity. These algorithms can navigate the non-convex surfaces effectively, ensuring that the unit modulus constraint is met while optimizing the overall system performance.

On this hand, some works approached the manifold-based algorithms for solving different problems related to the RIS-assisted communications systems. Table 1 highlights three wireless optimization examples deploying MO approach. In [1], the authors proposed a method to maximize EE by jointly optimizing the beamforming at the RIS and BS. The Riemann conjugate gradient (RCG) method was utilized to find solutions on the sphere for active beamforming and on the complex circle manifold (CCM) for passive beamforming. Similarly, in [2], the authors used the RCG method to optimize both active and passive precoding. However, this paper employed the CCM and oblique manifold. In [8], the authors aimed to optimize passive beamforming to nullify interference between the UEs completely. They demonstrated that the solution for this purpose lies on the Stiefel manifold.

Additionally, several works adopted the RCG method to optimize RIS passive beamforming aiming to maximize some KPI in RIS-enabled systems [3]–[7]. Reference [10] provides insights into how MO techniques are applied to solve resource allocation problems in B5G systems, i.e., near-field resource allocation for XL-MIMO systems, by comparing different methodologies and optimization tools for the beamforming design, including Riemannian MO, alternating optimization (AO), reinforcement learning, and a generative artificial intelligence-based method.

**Integrating RIS and non-orthogonal multiple access (NOMA) in mMIMO systems:** The MU RIS-aided uplink (UL) NOMA design is challenging since it requires joint optimization of both the transmit powers and the RIS reflection coefficients. Because the optimization variables are linked, the problem cannot be solved with a closed-form approach; also, it is a non-convex problem.

Existing solutions in the literature for UL RIS-NOMA design use the semidefinite programming (SDP) method to turn the optimization problem into a convex form that can be solved with convex programming tools. However, SDP-based approaches have high complexity, of order  $\mathcal{O}(N^{3.5})$ , especially when the number of RIS elements  $N$  is high, which renders these solutions unsuitable for IoT applications, where the BS may have limited power resources that cannot accommodate very complex tasks.

To reduce the complexity, the authors of [9] suggest a simple but effective alternating MO algorithm that works well for IoT applications that run on batteries. An alternating MO-based algorithm has been proposed for solving the phase shifts, analog beamforming, and transmit beamforming in RIS-aided UL NOMA, and compared with the successive convex approximation (SCA)-based method. Numerical results reveal that the proposed manifold alternating MO-based algorithm outperforms the existing schemes when the sum rate is optimized. A MO approach aims to provide a low-complexity design with powerful performance.

In [11], the authors investigate the role of RIS in enhancing the sum throughput for NOMA IoT networks. It proposes a novel resource allocation strategy that optimizes both time allocation and phase shift matrices during wireless energy transfer and wireless information transfer phases, respectively. The strategy employs *elements collaborative approximate* and *manifold space gradient descent* algorithms for optimization, demonstrating significant performance gains in simulated environments when compared to networks without RIS or using other resource allocation methods.

Authors in [12] explore RIS-aided NOMA in the UL of energy-limited networks. Two optimization problems are addressed: minimizing users' transmit power and maximizing EE. Joint optimization of users' transmit powers and RIS beamforming coefficients is achieved using a novel low-complexity algorithm on a CCM. To solve them, the author deploys iterative AO algorithms in two steps to jointly optimize the transmit powers of the users and the phase

shifts at RIS, under transmit power and Quality of Service (QoS) constraints: *i*) passive beamforming coefficients are used to solve the transmit power optimization problem. *ii*) fixes users' transmit powers and then solves the RIS coefficients optimization problem. Compared to three conventional SDP-based benchmarks, the proposed MO-based algorithm demonstrates better performance with reduced computational complexity, particularly when user target data rates are high.

## B. MOTIVATION AND CONTRIBUTION

This paper discusses the difficulties of finding the best solutions to non-convex problems in RIS-assisted mMIMO systems, mainly those that arise because passive RIS elements have a unit modulus constraint. Also, this work provides a more efficient and practical approach to solving complex optimization problems in advanced wireless communication systems compared to conventional methods. Hence, we need to leverage the geometric properties of manifolds for better solutions to wireless communication optimization problems. Finally, we address handling high-dimensional data often present in wireless communication systems.

The paper's contributions are as follows:

- ◆ The paper provides a tutorial on MO techniques and their applications in wireless communications systems.
- ◆ It explores five application examples in RIS-aided mMIMO systems, focusing on a) fairness; b) EE maximization; c) intra-cell pilot reuse interference mitigation; d) grant-free random access
- ◆ The paper demonstrates the effectiveness of MO methodology in these specific applications.
- ◆ It provides a framework for applying MO to wireless communication problems, including steps for identifying appropriate manifolds and formulating problems.
- ◆ The paper compares MO methods with alternative optimization techniques, highlighting MO's advantages in handling non-convex constraints and exploiting geometric properties.
- ◆ It presents a catalog of gradient descent-based algorithms adapted for manifold optimization.
- ◆ The paper provides detailed case studies on real-life problems using MO in RIS-aided mMIMO situations.

The motivations and contributions of this paper are significant in advancing the understanding and application of manifold optimization techniques in the context of modern wireless communication systems, particularly those involving RIS and mMIMO technology.

## C. ORGANIZATION OF THE PAPER

The remaining content of the article is organized as follows. Section II provides an overview of the manifold concept with alternatives for its application and its fundamental tools, and lists a bunch of usual manifolds. Section III structures the steps and selection of suitable manifold learning techniques, identifying key constraints and establishing the geometric

structure of these constraints as manifolds. Section IV discusses the main steps in formulating and solving wireless communication problems using the MO framework. Section V develops a practical optimization example in RIS-aided mMIMO systems; it also provides a catalog of gradient descent-based algorithms. Section VI provides a detailed case study on four real-life problems using MO. In this central part of the paper, four real-life uses of MO in RIS-aided mMIMO situations are discussed in detail. These include making networks fairer, making IoT systems more energy efficient, and allowing intra-cell pilot reuse. The MO-based complete solutions for the four real applications in wireless RIS-aided mMIMO systems are provided. Finally, Section VII draws the main conclusion and perspectives on the MO for wireless communication applications. The paper concludes with a summary of the findings and suggestions for future research directions.

## II. MANIFOLD FUNDAMENTALS

In this section, we start by highlighting different alternatives to the MO technique. In the subsequent subsection, we explain the manifold optimization framework. Finally, we catalog a list of manifolds found in many different real-world problems.

### A. ALTERNATIVES TO MANIFOLD OPTIMIZATION TECHNIQUE

There are some alternatives for solving non-convex optimization problems, including *heuristic evolutionaries* (HEMs), *convex relaxation* techniques, machine-learning (ML)-based algorithms, and *gradient-based* methods. **HEMs**, such as genetic algorithm (GA), particle swarm optimization (PSO), and simulated annealing (SA), among others, are capable of performing a global search and are less likely to get trapped in local minima, therefore, being suitable to be applied to a wide range of problems without requiring gradient information, however, they present demerits of *a)* computationally intensive, often requiring many function evaluations, making them computationally expensive; *b)* lack of guarantees of convergence to the global optimum and can be slow to converge.

The merits of **convex relaxation** techniques, such as SDP, and convex-concave procedure (CCP), include *a)* rigorous framework for approximating non-convex problems into convex ones, and *b)* polynomial-time solvability. However, these techniques suffer scalability issues, rapidly becoming computationally infeasible for large-scale problems; moreover, the quality of the solution provided by SDP and CCP depends on how well the non-convex problem can be approximated by a convex one.

Besides, **ML-based algorithms** can present impressive results since it can deal with large-scale problems, providing sub-optimal solutions. However, their feasibility in real-world scenarios is often limited. This limitation arises because many ML-based algorithms require an offline train-

ing stage (particularly neural networks (NNs) in supervised learning), utilizing data collected from real-world scenarios, however, it can be incompatible with the highly dynamic nature of wireless communication environments. The necessity for constant adaptation in these environments makes it challenging to rely on pre-trained models. Therefore, their practical application in wireless communications remains constrained by these real-world considerations.

Finally, **gradient-based** methods, such as *gradient descent*, *Newton's method*, and *conjugate gradient*, represent a competitive alternative to the MO approach for problems where gradient information is available, revealing strong local convergence properties in such scenarios. However, gradient-based methods can easily get trapped in local minima. As a substantial limitation, these methods require the objective function (OF) to be differentiable, which can not be always practical.

The key **pros** and **cons** of MO over traditional optimization methods in wireless communications are summarized in Table 2, and include *a)* natural handling of non-convex constraints; *b)* geometric property exploitation; *c)* local linearization; *d)* versatility in handling constraints and symmetries; and *e)* high-dimensional data management: Wireless communication systems often deal with high-dimensional data. Therefore, MO methods can transform this data into a more manageable form, improving signal processing and resource allocation optimization.

### B. MANIFOLD OPTIMIZATION FRAMEWORK

In an optimization framework, we consider the search space  $\mathcal{S}$  as the set containing all possible answers to our problem, and a cost function  $f : \mathcal{S} \rightarrow \mathbb{R}$  which associates a cost  $f(x)$  to each element  $x$  of  $\mathcal{S}$ . The goal is to find  $x \in \mathcal{S}$  such that  $f(x)$  is minimized:

$$\arg \min_{x \in \mathcal{S}} f(x). \quad (1)$$

We occasionally wish to denote the subset of  $\mathcal{S}$  for which the minimal cost is attained. We should keep in mind that this set might be empty.

The Euclidean structure of  $\mathbb{R}^n$  and the OF  $f$ 's smoothness are irrelevant to the optimization problem's definition. They are merely structures that we should use algorithmically to our advantage. Assuming linearity, the MO approach requires smoothness as the key structure to exploit.

#### 1) Optimization Over Smooth Surfaces

Manifolds are a fundamental concept in mathematics, particularly in geometry and topology. Manifolds provide a generalization of shapes and spaces that locally resemble Euclidean space. Indeed, optimization on manifolds is a versatile framework for continuous optimization. It encompasses optimization over vectors and matrices and allows optimizing over curved spaces to handle constraints and symmetries such as orthonormality, low rank, positivity, and invariance under group actions [13].



TABLE 2: Comparison of MO methods to its alternatives

Method	Pros	Cons
<b>MO</b>	<i>Handling Non-Convex Constraints:</i> MO methods naturally handle non-convex constraints by treating the problem as an optimization over a smooth manifold.	<i>Complexity in Implementation:</i> Implementing MO methods can be complex due to the need for specialized knowledge in differential geometry and manifold theory.
	<i>Exploiting Geometric Properties:</i> MO methods leverage the geometric properties of the problem, handling constraints and symmetries (orthonormality, low rank, positivity, and invariance), allowing for more efficient solutions.	<i>Algorithmic Design Challenges:</i> The manifold constraint adds complexity to the algorithmic design and theoretical analysis.
	<i>Local Linearization:</i> Manifolds are locally Euclidean, enabling linear optimization techniques in a more generalized form.	<i>Computational Overhead:</i> While efficient, MO methods can still be computationally intensive, especially for high-dimensional problems.
	<i>High-Dimensional Data Management:</i> MO methods can transform high-dimensional data into a more manageable form, improving optimization in tasks like signal processing and resource allocation.	
<b>HEMs</b>	<i>Global Search Capability:</i> These methods perform a global search and are less likely to get trapped in local minima.	<i>Computationally Intensive:</i> They often require many function evaluations, making them computationally expensive.
	<i>Flexibility:</i> They can be applied to various problems without requiring gradient information.	<i>Lack of Guarantees:</i> No guarantee to converge to the global optimum or can converge slowly.
<b>Convex Relaxation Techniques</b>	<i>Mathematical Rigor:</i> These methods provide a rigorous framework for approximating non-convex problems.	<i>Approximation Quality:</i> The quality of the solution depends on how well the non-convex problem can be approximated by a convex one.
	<i>Polynomial-Time Solvability:</i> Convex problems can be solved efficiently using polynomial-time algorithms.	<i>Scalability Issues:</i> These methods can become computationally infeasible for large-scale problems.
<b>ML-based algorithms</b>	<i>Adaptability:</i> ML methods can adapt to various scenarios and data patterns without requiring explicit modeling of the underlying physical processes.	<i>Training Data Requirement:</i> ML methods require large amounts of high-quality training data, which may not always be available or easy to obtain.
	<i>Data-Driven:</i> ML methods leverage large datasets to learn and improve performance over time, making them suitable for environments where data is abundant.	<i>Computational Complexity:</i> Training ML models, especially deep learning models, can be computationally intensive and time-consuming.
	<i>Automation:</i> Once trained, ML models can automate complex decision-making processes, reducing the need for manual intervention.	<i>Generalization:</i> ML models may struggle to generalize well to unseen scenarios or out-of-distribution data, leading to suboptimal performance.
	<i>Scalability:</i> ML algorithms can handle high-dimensional data and scale well with the increasing complexity of wireless communication systems.	<i>Interpretability:</i> Particularly deep NN, often act as black boxes, making it difficult to interpret/understand their decision-making processes.
<b>Gradient-Based Methods</b>	<i>Efficiency:</i> These methods are efficient for problems where gradient information is available.	<i>Requirement of Smoothness:</i> These methods require the OF to be differentiable.
	<i>Local Convergence:</i> They have strong local convergence properties.	<i>Local Minima:</i> They can easily get trapped in local minima.

Let us consider the set  $\mathcal{M}$  as a smooth manifold, and the function  $f$  is smooth on  $\mathcal{M}$ . Optimization over such surfaces can be understood as constrained because  $x$  is not free to travel in  $\mathbb{R}^n$  space but is only allowed to stay on the surface. The favored alternative viewpoint, in this case, is to consider this as unconstrained optimization in a universe where the smooth surface is the only thing that exists. As a result, the generalized Euclidean methods from

unconstrained optimization can be applied to the larger class of optimization over smooth manifolds. We require a correct knowledge of gradient and Hessian on smooth manifolds to generalize techniques such as gradient descent and Newton’s method. In the linear instance, this requires including an inner product or Euclidean structure. In a more general situation, it is advisable to exploit the property that smooth manifolds are locally linearizable around all points.

The linearization at  $x$  is the tangent space. Giving each tangent space its inner product<sup>1</sup> transforms the manifold into a Riemannian manifold (RM), upon which we construct what is known as a Riemannian structure [13], [14].

## 2) Operators on Riemannian Manifold

RMs are mathematical objects that generalize the notion of Euclidean space to more complex and curved geometries. These spaces are foundational in various fields, including optimization, differential geometry, and theoretical physics [15]. A Riemannian manifold is locally similar to Euclidean space but differs in that it is equipped with a Riemannian metric tensor. This tensor defines the distances and angles between points on the manifold by assigning a positive definite inner product to each tangent space. This inner product allows for the measurement and interpretation of geometric properties such as length, angle, and curvature. Some key definitions and concepts in Riemannian geometry include:

- ◇ Riemannian Gradient ( $\nabla_{\mathcal{M}}f(\mathbf{x})$ ): This is the generalization of the gradient from Euclidean space  $\nabla f$  to Riemannian manifolds. Specifically, the Riemannian gradient of a function  $f$  on a manifold  $\mathcal{M}$  is the projection of the Euclidean gradient onto the tangent space of the manifold at a given point.

$$\nabla_{\mathcal{M}}f(\mathbf{x}) = P_{\mathcal{T}_x\mathcal{M}}(\nabla f(\mathbf{x})), \quad (2)$$

where  $P_{\mathcal{T}_x\mathcal{M}}$  is the projection operator onto the tangent space  $\mathcal{T}_x\mathcal{M}$ . It represents the direction of the steepest ascent of a function  $f$  on the manifold  $\mathcal{M}$ .

- ◇ Retraction Operation ( $\text{Retr}_{\mathcal{M}}(\mathbf{x})$ ): The retraction operator  $\text{Retr}_{\mathcal{M}}(\mathbf{x})$  of a point on a manifold  $\mathcal{M}$  is the projection of the given point  $\mathbf{x}$  over the manifold  $\mathcal{M}$ . Retractions are used to ensure that optimization steps remain on the manifold.

The Riemannian gradient and retraction operation are essential for algorithms that optimize manifolds, as they ensure that the iterative steps respect the manifold's geometric structure. Moreover, we should bear in mind that each manifold has its own projection operator on the tangent space, as well as the retraction operator.

## 3) Challenges in Manifold Optimization

If additional constraints other than the manifold constraint are applied, one can add an indicator function of the feasible set of such additional constraints in the OF. Hence, the optimization problem covers a general formulation for MO. Moreover, the manifold constraint is one of the main difficulties in algorithmic design and theoretical analysis.

One of the main challenges in MO usually is the non-convexity of the manifold constraints. By utilizing the ge-

<sup>1</sup>Varying smoothly with  $x$  in a way to be determined precisely.

ometry of the manifold, a large class of constrained optimization problems can be viewed as unconstrained optimization problems on the manifold [16].

## C. COLLECTION OF MANIFOLDS

Optimization on manifolds is a versatile framework for continuous optimization. It encompasses optimization over vectors and matrices and adds the possibility to optimize over curved spaces to handle constraints and symmetries such as orthonormality, low rank, positivity, and invariance under group actions.

One of the most common manifolds is the **CCM**, in which all the elements of the optimization variable should have a unit modulus. This is usually the case of RIS phase shift optimization problems under passive operation mode. Hence, the MO framework is well-suited for the RIS problems. Table 3 summarizes the common real and complex types of manifolds, with particular emphasis on the complex circle manifold, also known as the “complex one-manifold”.

A *complex manifold* is a manifold with a structure that locally resembles complex Euclidean space, *i.e.*,  $\mathbb{C}^n$ . This means a neighborhood is homeomorphic around every point to an open subset of  $\mathbb{C}^n$ . In particular, Table 4 shows the main features and applications of the Complex Circle ( $\mathcal{S}^1$ ) manifold.

Notice that the complex circle  $\mathcal{S}^1$  is a crucial introductory example of manifolds and complex manifolds, offering valuable insights into higher-dimensional and more complex spaces used in various mathematical and physical applications. Huge practical applications deploy MO in real-life communications systems. In the sequel, we present five classes of RIS-aided mMIMO system applications involving MO.

## III. MANIFOLD LEARNING METHODS AND STRUCTURES

Specific problems within wireless communication scenarios possess unique domains, characteristics data, and different properties. To effectively capture the essential structure of the data and optimize the performance of the wireless system, it is crucial to thoroughly understand the problem. It is important to note that the associated manifold can vary significantly from one problem to another, depending on the inherent characteristics of each situation and requirements.

By appropriately understanding the associated manifold, one can effectively leverage manifold learning techniques to transform high-dimensional data into a more manageable form, leading to better optimization in wireless systems. In the context of practical wireless system problems, manifold techniques and optimization can be employed to effectively model complex, high-dimensional spaces and enhance performance in various tasks such as signal processing, resource allocation, and network management.

TABLE 3: Common collection of manifolds [14]

Manifolds	Feature
<b>Euclidean Space</b> $\mathbb{R}^n$	$\mathbb{R}^n$ is the most straightforward example of a manifold, where each point has a local neighborhood that looks exactly like $\mathbb{R}^n$ . Flat, infinite extent, commonly used in most basic analyses.
<b>Circle</b> ( $S^1$ )	$S^1$ represents a one-dimensional manifold (1-manifold), which can be thought of as points equidistant from a center point in 2D space, like the perimeter of a circle; intrinsic periodicity (models cyclical phenomena).
<b>Sphere</b> ( $S^n$ )	$S^n$ generalizes the concept of a circle and sphere to “ $n$ ” dimensions; e.g., $S^2$ is the 2D surface of a 3D ball. Compact, without boundary, intrinsic higher-dimensional analogs. <b>Use Cases:</b> Modeling surfaces like Earth’s surface ( $S^2$ ).
<b>Torus</b> ( $T^2$ )	The 2D torus is a surface shaped like a donut, which can be defined as $S^1 \times S^1$ , the product of two circles or, generalizing, a product of $n$ circles, closed and compact. <b>Use Cases:</b> Modeling periodic boundary conditions, complex cyclical phenomena
<b>Projective Space</b> $\mathbb{R}P^n$	Space of lines through the origin, compact, involves projective transformation. <b>Use Cases:</b> Computer vision, robotics, projective geometry.
<b>Hyperbolic Space</b> $\mathbb{H}^n$	Non-Euclidean, negatively curved. <b>Use Cases:</b> Representing hierarchical tree structures, complex networks.
<b>Hyperplanes</b>	These are generalizations of planes in higher dimensions.
<b>Lie Groups:</b>	Smooth manifold that is also a group, with applications in physics and engineering. <i>Examples:</i> $SO(3)$ , $SU(2)$ . <b>Use Cases:</b> Robotics, control theory, representation of symmetries.
<b>Grassmannian</b> ( $G(k, n)$ )	Space of all $k$ -dimensional subspaces of an $n$ -dimensional vector space. <b>Use Cases:</b> Signal processing, principal component analysis in higher dimensions.
<b>Stiefel Manifold</b> ( $V(k, n)$ ):	Space of all orthonormal $k$ -frames in $n$ -space. <b>Use Cases:</b> Multivariate statistics, optimization on orthonormal matrices.
<b>Kähler Manifold:</b>	A complex manifold with a Hermitian metric, deeply tied to complex and symplectic geometry. <b>Use Cases:</b> Theoretical physics, string theory.
<b>Calabi-Yau Manifold:</b>	A special type of Kähler manifold with a Ricci-flat metric. <b>Use Cases:</b> String theory, particularly compactification methods.
<b>Complex Manifolds</b>	
<b>Complex Circle</b> ( $S^1$ )	or <i>Complex 1-Manifold</i> : identified with the complex circle; defined as the set of all complex numbers of the unit norm, defined as: $S^1 = \{z \in \mathbb{C} \mid  z  = 1\}$ . Here, $ z $ denotes the modulus of the complex number $z$ . Manifolds modeled on complex numbers, allowing holomorphic coordinates. <b>Use Cases:</b> Complex dynamics, algebraic geometry.

**A. STEPS FOR IDENTIFY A MANIFOLD**

- 1) *Identifies the Problem Domain and Requirements:* Common problems in 5G/B5G include beamforming, interference management, user scheduling, and power control. Therefore, identifying the specific requirements and constraints such as latency, throughput, EE, and QoS, is essential.
- 2) *Analyze the Data:* Collect and analyze the data relevant to the optimization problem, including signal measurements, user mobility patterns, channel state information (CSI), and network topology.
- 3) *Understand the Dimensionality:* Determine the intrinsic dimensionality of the data. High-dimensional datasets often have a lower-dimensional structure that can be exploited. Use principal component analysis (PCA) or exploratory data analysis to estimate the true dimensionality of the data.
- 4) *Identify an Appropriate Manifold Learning Technique* [17]:
  - ◊ **Principal Component Analysis (PCA):**. This linear technique reduces dimensionality while re-

taining the maximum variance in the data. *Use Cases:* Effective for datasets where the important variance is linear and global structure is more important.

- ◊ **Multidimensional Scaling (MDS):** Can be either linear or non-linear, and aims to preserve pairwise distances. *Use Cases:* Good for visualizing distances or dissimilarities among data points.
- ◊ **Isometric Mapping (Isomap):** Non-linear and preserves global geodesic distances, useful when the data lies on a curved surface; suitable for data on a nonlinear manifold. *Use Cases:* Data where the intrinsic geometry is best captured by a global isometry.
- ◊ **Locally Linear Embedding (LLE):** Effective for capturing local neighborhood information, useful in highly curved manifolds. It preserves local neighborhood structure using linear reconstructions. *Use Cases:* Capturing local manifold structure, suitable for highly curved manifolds.
- ◊ **t-Distributed Stochastic Neighbor Embedding (t-SNE):** Often used to visualize high-dimensional

TABLE 4: Features and applications for the complex circle ( $\mathcal{S}^1$ ) manifold

Feature	Description
<b>1-Dim.</b>	While being embedded in $\mathbb{C}$ (which is like $\mathbb{R}^2$ ), the complex circle $\mathcal{S}^1$ is a 1-dimensional manifold.
<b>Compactness</b>	It is a closed and bounded subset of $\mathbb{C}$ .
<b>Local Structure</b>	Locally, around any point on $\mathcal{S}^1$ , it resembles the real line $\mathbb{R}$ , meaning it can be mapped one-to-one onto an open interval of $\mathbb{R}$ .
<b>Visualization</b>	One can visualize $\mathcal{S}^1$ as the unit circle in the complex plane, where each point on the circle is defined by a complex number $z$ with $ z  = 1$ . This can be parameterized as $z = e^{i\theta}$ for $\theta \in [0, 2\pi)$ , capturing its circular nature.
<b>Complex Structure</b>	Looking at local coordinates as a complex manifold using complex logarithms and exponential. These give the local diffeomorphisms needed to open up parts of $\mathbb{C}$ . The manifold structure is given by charts that map intervals around each point to the Euclidean space $\mathbb{C}$ .
APPLICATIONS OF THE COMPLEX CIRCLE MANIFOLD	
<b>Topology</b>	Understanding the structure and properties of $\mathcal{S}^1$ is fundamental in algebraic topology, which contributes to studying fundamental groups and covering spaces.
<b>Complex Structure</b>	$\mathcal{S}^1$ is the natural domain for periodic functions and is central in studying Fourier analysis.
<b>Physics</b>	The complex circle appears in various physical theories, including quantum mechanics and wave mechanics, describing spaces of phases.

data visualization, capturing local similarities. Non-linear and focuses on preserving local similarities. *Use Cases:* Visualization of high-dimensional datasets, often used in exploratory data analysis.

- ◊ **Uniform Manifold Approximation and Projection (UMAP):** Non-linear, faster, and more scalable than t-SNE, preserves local and global structures. *Use Cases:* Similar use cases as t-SNE but with better scalability and speed.
- ◊ **Laplacian Eigenmaps:** Non-linear, relies on graph-based representation, preserves local neighborhood information. *Use Cases:* Data where local connectivity and local geometrical features are important.
- ◊ **Autoencoders:** Non-linear, based on neural networks, encodes data into latent spaces. *Use Cases:* Data with complex non-linear structures, can be used for both unsupervised and supervised learning.
- ◊ **Hessian Eigenmaps:** Non-linear, focuses on preserving second-order structure (curvatures). *Use*

*Cases:* Manifolds where curvature information is crucial.

- ◊ **Diffusion Maps:** Non-linear, uses diffusion processes to find meaningful geometric descriptions. *Use Cases:* Clustering, spectral embedding, data denoising.
- 5) *Implement and Validate:* Implement the chosen manifold learning technique using frameworks such as `scikit-learn` or custom-built solutions. Thus, validating the manifold representation by examining how well it captures the critical features of the data and supports the optimization objectives, can be done. Use cross-validation or other validation techniques to ensure the manifold model generalizes well to new data.
  - 6) *Apply for Optimization:* Once the manifold is identified and validated, use it to transform and simplify the optimization problem, accordingly: for example, **Beamforming** (manifold learning can help reduce the complexity of beam selection and improve beam alignment); **Resource Allocation** (utilize manifold structures to identify clusters of users or resources to optimize allocation strategies); **Interference Management** (capture interference patterns' spatial and temporal characteristics on lower-dimensional manifolds).

#### IV. METHODOLOGY FOR FORMULATING AND SOLVING OPTIMIZATION PROBLEMS WITH MANIFOLDS

In the following, we illustrate the MO methodology by detailing the steps involved in addressing a real-world problem in communication systems. Specifically, we will focus on optimizing phase shifts in a RIS using manifold optimization techniques. This approach serves as an example, but the methodology can be applied to any problem involving non-convex constraints that can be represented as a manifold. RIS is conceived to modify the propagation environment to create constructive interference patterns dynamically, thus, in practice enhancing signal strength at the UEs, e.g., IoT devices, can be very interesting. The phase shifts introduced by RIS elements and the configurations of the mMIMO antenna arrays constitute high-dimensional and non-linear spaces. MO provides a framework for handling these complex optimization problems.

##### STEP 1: PROBLEM FORMULATION

- ◊ **Define the Objective:** Clearly define the optimization problem in terms of an OF. This could be maximizing some KPI, such as spectral efficiency (SE), EE, or signal-to-noise ratio (SNR). The OF is represented by  $f(\theta, \mathbf{h})$ , where  $\mathbf{h}$  and  $\theta$  represent the channel gain and the phase shift imposed by the RIS, equipped  $N$  elements, respectively, with  $[\theta]_n = \alpha_n e^{j\theta_n}$ .
- ◊ **Constraints:** Identify the constraints of the problem, such as power limitations, RIS phase shift constraints,



and CSI requirements. In our example, physically, each element in the passive RIS must satisfy the following property  $|\alpha_n e^{j\theta_n}| = 1$ .

### STEP 2: IDENTIFY THE MANIFOLD STRUCTURE

- ◇ **Manifold Description:** Establish the geometric structure of the constraint. For instance, RIS phase shifts lie on CCM, which can be treated as a manifold<sup>2</sup> and described as

$$\mathcal{S}^1 = \{e^{j\theta_n} \in \mathbb{C} \mid \theta \in [0, 2\pi)\}, \quad \forall n = 1, \dots, N, \quad (3)$$

where  $N$  is the total number of elements of RIS.

### STEP 3: REFORMULATE THE OPTIMIZATION PROBLEM

- ◇ **Manifold Representation:** Reformulate the constraint problem regarding manifold constraints. For example, if the optimization involves unit-modulus constraints, e.g., RIS phase shifts  $\theta \in [0, 2\pi)$ , represent these in terms of the complex exponential form  $e^{j\theta}$ . In our specific example, the optimization problem becomes:

$$\max_{\theta \in \mathcal{S}^1} f(\theta, \mathbf{h}), \quad (4)$$

where,  $\theta$  is a vector of phase shifts, and each element must satisfy the unit-modulus constraint.

- ◇ **Alternative Parameterization:** Use appropriate parameterizations to represent elements on the manifold in a computationally friendly way.

### STEP 4: DEVELOP AN OPTIMIZATION ALGORITHM

- ◇ **Initialization:** Start with an initial feasible point on the manifold. This might involve random initialization or a heuristic-based initialization.

$$\theta^{(0)} = [\theta_1^{(0)}, \theta_2^{(0)}, \dots, \theta_N^{(0)}]^T. \quad (5)$$

- ◇ **Gradient Descent:** Use some *manifold-based optimization technique* (see subsection B of section V) to iteratively update the phase shifts and move towards the local optimum. The steps should ensure the updated points lie on the manifold.

$$\theta^{(k+1)} = \theta^{(k)} + \alpha \nabla_{\mathcal{M}} f(\theta^{(k)}), \quad (6)$$

where  $\alpha$  is the step size and  $\nabla_{\mathcal{M}} f(\theta^{(k)})$  is the Riemannian gradient at the  $k$ -th iteration.

- ◇ **Returning to the Manifold:** After updating the phase shifts, the updated point should be on the manifold surfaces, therefore, the retraction operator should be applied. Specifically, for the CCM manifold, the retraction operator is given as

$$\text{Retr}_{\mathcal{S}^1}(\theta^{(k+1)}) = \frac{\begin{bmatrix} \theta^{(k+1)} \\ \vdots \\ \theta^{(k+1)} \end{bmatrix}_n}{\left\| \begin{bmatrix} \theta^{(k+1)} \\ \vdots \\ \theta^{(k+1)} \end{bmatrix}_n \right\|}, \quad \forall n = 1, 2, \dots, N. \quad (7)$$

### STEP 5: ITERATIVE OPTIMIZATION

- ◇ **Iterative Process:** Iterate the optimization process until convergence. The stopping criterion could be based on the change in the OF value or the gradient norm at the  $k$ -th iteration till a small positive threshold  $\epsilon$ .

$$\|\nabla_{\mathcal{M}} f(\theta^{(k)})\| < \epsilon. \quad (8)$$

### STEP 6: VALIDATION AND PERFORMANCE EVALUATION

- ◇ **Validation:** Validate the optimized phase shifts by evaluating the reflected RIS signal's energy. Compare the performance with traditional optimization methods to demonstrate the efficiency and effectiveness of the MO-based approach.

## V. PRACTICAL EXAMPLE AND GRADIENT DESCENT-BASED ALGORITHMS

In this section, we elucidate a practical example of RIS-assisted solved by MO in wireless communication systems. In the following, we exhibit a list of gradient descent-based methods, which can be generalized to the Riemannian space and utilized in MO strategy.

### A. EXAMPLE: BS PRECODING AND RIS PHASE SHIFT OPTIMIZATION

Consider optimizing the beamforming weights at BS and RIS phase shifts to maximize the sum of signal-to-interference-plus-noise ratios (SINRs). Following the steps elucidated in Section III, we can effectively solve the precoding and RIS phase shift optimization problem using MO techniques. The key advantage of this approach is its ability to handle non-convex constraints naturally, leading to more efficient and effective optimization than more conventional methods. We start, by formulating our **objective**, which is to optimize the active beamforming at the BS (equipped with  $M$  antennas) and the passive reflective beamforming at the RIS to maximize the SINR of  $K$  UEs. This joint problem can be formulated as:

$$\max_{\mathbf{W}, \theta} f(\theta, \mathbf{W}) \triangleq \sum_{k=1}^K \frac{|\mathbf{w}_k^H \mathbf{h}_k(\theta)|^2}{\sum_{j \neq k} |\mathbf{w}_j^H \mathbf{h}_k(\theta)|^2 + \sigma^2}, \quad (9a)$$

$$\text{subject to } \theta \in \mathcal{S}^1, \quad (9b)$$

$$\text{tr}(\mathbf{W}^H \mathbf{W}) \leq P_{\max}, \quad (9c)$$

where  $\sigma^2$  is the noise power. The **constraints** for the adopted problem are related to the RIS phase shifts  $\theta$ , as shown in Eq. (9b), which should lie on the unit complex circle ( $|e^{j\theta_i}| = 1, \forall i$ ), and about the active beamforming vector  $\mathbf{W}$ , which should satisfy power norms, i.e., it must not

<sup>2</sup>Common manifolds in wireless communications include the Stiefel manifold (for orthonormal matrices) and the Grassmann manifold (subspaces). For a complete list of Manifolds, see Table 3.

exceed the available power budget at the BS ( $P_{\max}$ ), as described in Eq. (9c).

The optimization problem above can be addressed using MO. By treating the beamforming weights and RIS phase shifts as optimization variables on a product manifold of spheres and circles, we identify the manifold structure, therefore, the active beamforming matrix  $\mathbf{W}$  lies on a Stiefel manifold (for orthonormal matrices), and the phase shifts  $\boldsymbol{\theta}$  lie on a CCM  $S^1$ . These manifolds can be described as:

$$\mathcal{M}_W = \{\mathbf{W} \in \mathbb{C}^{M \times K} \mid \mathbf{W}^H \mathbf{W} = \mathbf{I}_K\}, \quad (10)$$

$$\mathcal{M}_\theta = \{e^{j\theta} \in \mathbb{C} \mid \theta \in [0, 2\pi)\}. \quad (11)$$

With the given step, we can reformulate the optimization problem in terms of the manifold constraints. The optimization problem becomes:

$$\max_{\mathbf{W} \in \mathcal{M}_W, \boldsymbol{\theta} \in \mathcal{M}_\theta, \mathbf{p}} f(\mathbf{W}, \boldsymbol{\theta}), \quad (12)$$

where  $\mathbf{p}$  is the power allocation corresponding to the UEs. Notice that  $\mathbf{p}$  emerges from the assumption, of  $\mathbf{W} \in \mathcal{M}_W$ , and its optimization is very consolidated in the literature.

The **initialization** of the algorithm can start with an initial feasible point on the manifold. This could be a random initialization or based on a heuristic:

$$\mathbf{W}^{(0)}, \boldsymbol{\theta}^{(0)}. \quad (13)$$

Thus, the Riemannian gradient descent to iteratively update the beamforming matrix and phase shifts. The update rule involves computing the Riemannian gradient and ensuring the updated points lie on the manifold.

$$\mathbf{W}^{(k+1)} = \mathbf{W}^{(k)} + \alpha_W \nabla_{\mathcal{M}_W} f(\mathbf{W}^{(k)}, \boldsymbol{\theta}^{(k)}), \quad (14)$$

$$\boldsymbol{\theta}^{(k+1)} = \boldsymbol{\theta}^{(k)} + \alpha_\theta \nabla_{\mathcal{M}_\theta} f(\mathbf{W}^{(k)}, \boldsymbol{\theta}^{(k)}), \quad (15)$$

where  $\alpha_W$  and  $\alpha_\theta$  are the step sizes, and  $\nabla_{\mathcal{M}_W} f$  and  $\nabla_{\mathcal{M}_\theta} f$  are the Riemannian gradients.

The updated values should return to the manifold surfaces, and this can be done by applying the retraction operator

$$\mathbf{W}^{(k+1)} = \text{Retr}(\mathbf{W}^{(k+1)}), \quad (16)$$

$$\boldsymbol{\theta}^{(k+1)} = \text{Retr}(\boldsymbol{\theta}^{(k+1)}). \quad (17)$$

Finally, we can **iterate** the optimization process until convergence. The stopping criterion could be based on the change in the OF value or the gradient norm.

$$\|\nabla_{\mathcal{M}_W} f(\mathbf{W}^{(k)}, \boldsymbol{\theta}^{(k)})\| < \epsilon, \quad (18)$$

$$\|\nabla_{\mathcal{M}_\theta} f(\mathbf{W}^{(k)}, \boldsymbol{\theta}^{(k)})\| < \epsilon, \quad (19)$$

where  $\epsilon$  is a small positive threshold.

Thus, we can validate the optimized beamforming matrix and phase shifts by evaluating the SINRs. We should compare the performance with traditional optimization methods to demonstrate the efficiency and effectiveness of the manifold-based approach.

## B. GRADIENT DESCENT-BASED ALGORITHMS

Manifold-based optimization techniques include Riemannian Newton (RN), RCG, Riemannian Trust-Region (RTR), and Riemannian Gradient Descent (RGD). These techniques are powerful for optimizing functions constrained to manifolds, taking into account the non-Euclidean geometry of the optimization space. By leveraging the geometric properties of manifolds, these methods enable efficient and effective optimization. This is particularly beneficial in complex wireless communication systems, such as RIS-enabled mMIMO, where gradients are computed directly on the manifold, navigating over the curvature of the space. This approach ensures efficient convergence to locally optimal solutions.

**RGD:** The RGD is an optimization technique that extends the classical gradient descent method to Riemannian manifolds. The optimization process is constrained to a curved space rather than a flat Euclidean space. The key idea is to iteratively move towards the local optimum while ensuring that each update remains on the manifold. The RGD Algorithm steps are as follows:

- ◇ **Initialization:** Start with an initial feasible point on the manifold.
- ◇ **Gradient Computation:** Compute the Riemannian gradient, which is the projection of the Euclidean gradient onto the tangent space of the manifold.
- ◇ **Update Rule:** Move in the direction of the Riemannian gradient by a step size, ensuring the updated point lies on the manifold. This often involves a retraction operation that maps the point back onto the manifold.
- ◇ **Iteration:** Repeat the gradient computation and update steps until convergence.

---

### Algorithm 1 RGD Algorithm

---

- 1: **Input:** Initial point  $\mathbf{x}_0$  on manifold  $\mathcal{M}$ , step size  $\alpha$ , max iterations  $K$
  - 2: **Output:** Optimized point  $\mathbf{x}^*$  on the manifold // *Input and output specifications*
  - 3:  $k \leftarrow 0$  // Initialization of the iteration counter
  - 4: **while**  $k < K$  and not converged **do**
  - 5:   Compute Riemannian gradient  $\text{grad} f(\mathbf{x}_k)$  // *Project Euclidean gradient onto tangent space*
  - 6:   Update:  $\mathbf{x}_{k+1} \leftarrow \mathcal{R}_{\mathbf{x}_k}(-\alpha \text{grad} f(\mathbf{x}_k))$  // *Utilize retraction operator to map point back to manifold*
  - 7:    $k \leftarrow k + 1$
  - 8: **end while**
  - 9: **return**  $\mathbf{x}_k$  // *Return of the final optimized point*
- 

**RN:** RN method is an extension of the classical Newton's method to Riemannian manifolds. It uses second-order information (Hessian) to achieve faster convergence compared to the gradient descent.

**RCG:** RCG is an adaptation of the conjugate gradient method to Riemannian manifolds. It combines the efficiency of the

conjugated gradient method with the geometric constraints of manifolds.

*RTR*: RTR methods extend trust-region methods to the Riemannian manifolds. These methods iteratively solve a local approximation of the optimization problem within a “trust region” around the current point.

Utilizing Monte-Carlo Simulation (MCs) or other simulation techniques is useful to evaluate the algorithm’s performance under different scenarios. Based on simulation results, we can also refine the algorithm for better performance by adjusting parameters and re-evaluating. Refinement based on simulations is a critical step in the optimization process, especially when dealing with complex systems like those involving manifolds. In this context, the refinement process based on simulations might involve specific steps such as:

- ◇ *Gradient and Hessian Adjustments*: Fine-tuning the computation of Riemannian gradients and Hessians to ensure they accurately capture the manifold’s geometry.
- ◇ *Retraction Operations*: Modifying the retraction operations to better map updated points back onto the manifold.
- ◇ *Step Size Adaptation*: Adjusting the step size dynamically based on the manifold’s curvature to ensure efficient convergence.
- ◇ *Constraint Handling*: Refining how additional constraints are incorporated into the optimization problem, possibly by adjusting the indicator functions or penalty terms.

The goal is to iteratively improve the algorithm or model based on empirical evidence from simulations, leading to better performance in the target application. How refinement is typically done based on simulations is summarized in Algorithm 2.

Some open-source libraries support manifold structures, such as *Manopt tools*, which implements a bunch of manifold collections available on *Manopt* (Matlab) or *Pymanopt* (Python), which can be useful for obtaining solutions of many diverse problems [13], [14].

## VI. MANIFOLDS IN RIS-AIDED MASSIVE MIMO SCENARIOS: FOUR REAL APPLICATIONS

In the sequel, we discuss in detail four applications of MO framework to wireless communication systems, precisely, by applying different MO tools for RIS-aided mMIMO systems optimization. We use specific optimization tools based on MO procedures and methodologies, confirming the promising results attainable by applying MO tools.

Subsection A (*Application 1*) presents an efficient algorithm to maximize the minimum rate of the network. This algorithm enhances the system’s rate in a maximally fair manner by leveraging RCG within CCM. We then compare the performance and complexity of the proposed technique against benchmarks commonly used in the literature for RIS-assisted mMIMO, such as SCA and AO. The proposed algo-

---

### Algorithm 2 Refinement Based on Simulations

---

- 1: **Initial Simulation:**
  - 2: Run initial simulations to evaluate the performance of the current algorithm or system configuration.
  - 3: Collect performance metrics such as SE, EE, error rates, throughput, etc.
  - 4: **Performance Analysis:**
  - 5: Examine the simulation results to identify strengths and weaknesses.
  - 6: Determine which aspects are underperforming or causing issues.
  - 7: **Parameter Adjustment:**
  - 8: Modify parameters of the algorithm or system based on the analysis.
  - 9: Make necessary changes to the algorithm itself if required.
  - 10: **Re-simulation:**
  - 11: Perform new simulations with the adjusted parameters or modified algorithm.
  - 12: Compare the new simulation results with the previous ones.
  - 13: **Iteration:**
  - 14: Repeat the process of analysis, adjustment, and re-simulation multiple times.
  - 15: Continue iterating until performance metrics converge to satisfactory levels.
  - 16: **Validation:**
  - 17: Use cross-validation techniques to ensure generalization to different scenarios.
  - 18: Test the refined system under various conditions for robustness.
  - 19: **Final Tuning:**
  - 20: Perform fine-tuning of parameters to achieve the best possible performance.
  - 21: Use advanced optimization techniques if necessary.
- 

gorithm demonstrates significant gains over these benchmarks in terms of both performance and complexity.

Subsection B (*Application 2*) discusses how effective can be an RM-based RIS phase shift optimization method for optimizing the RIS phase shifts and the BS combining vectors. This technique is designed to minimize the UL transmit power of the UEs in the context of an IoT network supported by RIS. Initially, the joint optimization for the phase shift and combining vectors is formulated aiming to improve the overall system EE by minimizing the UL transmit power while guaranteeing a minimum QoS for the devices. To tackle the non-convexity of the problem, RM-based iterative alternating optimization (i-AO) technique was deployed. The RM iterative alternating optimization (RM-AO) algorithm greatly improves the system’s EE and *resource efficiency*<sup>3</sup> when compared to the non-RIS MU mMIMO system.

Subsection C (*Application 3*) discusses how to apply the MO framework to the RIS phase shifts optimization for intra-cell pilot reuse and the associated channel estimation. Relying upon the knowledge of only statistical CSI, the RIS phase shift optimization highlights the remarkable performance improvements achieved by the proposed scheme (for both UL and downlink (DL) transmissions).

---

<sup>3</sup>The SE × EE tradeoff.

Subsection D (*Application 4*) presents an optimization problem in a RIS-based GF random access (GF-RA) protocol, formulated to obtain a uniform high-gain reflected multi-beam in the intended direction while keeping low reflection gains in the unintended ones, subject to the unit modulus constraint. A MO framework reveals to be a promising tool to solve such optimization problems.

#### A. Application 1: Maximizing Fairness in RIS-Aided *m*-MIMO DL

To achieve efficient wireless communication, it is crucial to utilize available resources effectively, particularly in the context of future wireless networks. With the rise of the passive RIS, another variable should be appropriately optimized, the passive reflective beamforming. Jointly, the active precoding at the BS must not be overlooked. By leveraging advanced techniques, such as Zero-Forcing (ZF) precoding, we can achieve a condition where the total interference of the system can be completely nullified.

To accomplish this efficiently, accurate CSI is crucial. By knowing the CSI, the BS can effectively manage the system, by sending specific power for the UEs and configuring the RIS, to enhance the overall performance of the network. Besides, fairness in future wireless communications is fundamental since it can provide access for all UEs in the cell from an equality perspective. With the RIS assistance, there is more room for improving fairness, demanding thus research efforts to develop techniques to achieve such a challenging target.

We aim to fairly maximize the UEs' communication performance. To achieve this, we address the max-min fairness problem, focusing on maximizing the common SINR across all UEs. To this end, the reflective passive beamforming  $\theta$  at the RIS should be optimized, subject to the passive RIS constraints. We demonstrate that this problem can be formulated as a *minimization of inverse-summation of eigenvalues* of channel matrix under the complex circle manifold. Consequently, optimization tools such as manifold techniques, specifically, the RCG, can be appropriate for solving this problem, ensuring that the obtained solution remains within the manifold formed by the non-convex constraint.

**System Model and Problem Formulation:** Consider a MU *m*MIMO system operating in DL mode, with assistance of a RIS composed of  $N$  reflecting elements, where  $K$  single-antenna devices are served simultaneously by a BS equipped with  $M$  antennas, as illustrated in Figure 1a.

To solve the intended problem, we need to optimize the active beamforming at the BS ( $\mathbf{W}$ ) and the passive reflective beamforming at the RIS ( $\theta$ ). This problem involves two main constraints:

- Ensuring that the optimized active beamforming at the BS consumes no more than the available power budget ( $P_{\max}$ ).

- Ensuring that the optimized reflective passive beamforming obeys the passive constraint of the RIS, i.e., all elements should maintain the unit-modulus.

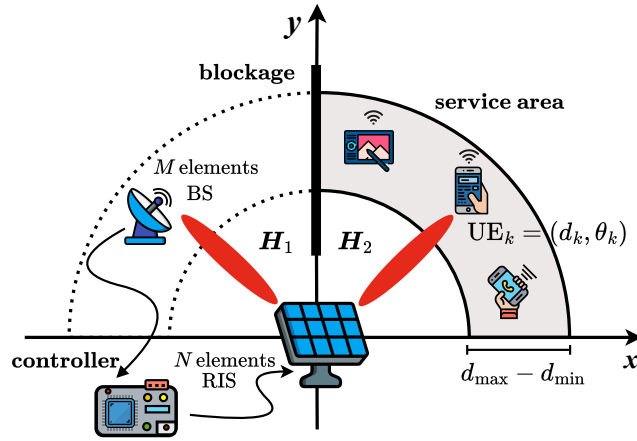
Some studies in the literature have already addressed the max-min problem, focusing on optimizing both active and passive beamforming. Solutions based on diverse techniques have been proposed, such as semidefinite relaxation (SDR) with SCA [18], penalty method followed by SCA [19], and even fractional programming (FP) with SCA [20]. It is noteworthy that all these techniques leverage from the AO, where this methodology is iterative and optimizes each variable of interest sequentially while keeping the others constant, and is repeated until convergence. Although all these works proposed different ways to convex the original non-convex max-min problem, proposing interesting sub-optimal solutions, their performance in real-world scenarios can be harmed due to their complexity. The main factor is that they suffer from high running time since they rely on CVX. Due to the interior point method implemented therein, this may lead to relatively high computational complexity. To further reduce the complexity and, consequently, the time processing, in the following, we propose a method of optimizing the minimum rate in a **two-step** process, which can considerably reduce the complexity and provide interesting performance gain, as we will see further ahead.

**Proposed Solution** The proposed solution has as the main factor avoiding the AO methodology, remarkably reducing the complexity. Therefore, to this end, the proposed effective approach to solving the max-min optimization problem consists of controlling each beamforming function separately, providing a two-step algorithm that does not rely on an iterative process. With this methodology, one can design active beamforming to provide the same SINR (denoted as  $\gamma$ ) for all the UEs, which we denote as **step 1** of the algorithm, while the following task, **step 2**, we concentrate on designing the passive beamforming aiming to maximize the common SINR. To be more specific:

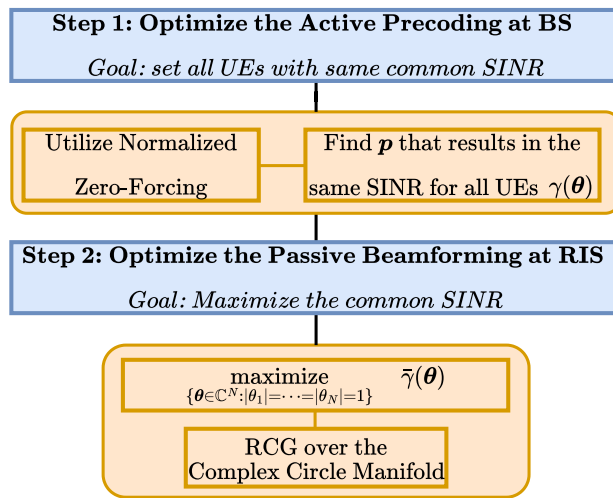
##### Step 1 – Optimizing the Active Precoding at BS:

- ◊ Find active precoding that can provide the same SINR condition among all the served UEs. To achieve this configuration, we provide the normalized ZF precoding, eliminating the interference suffered by the UEs. However, the normalized ZF does not guarantee the equal SINR conditions between the UEs; thus, the power allocation referring to each UE should be optimized yet, aiming to achieve the maximum fairness condition. Fortunately, the ZF precoding turns out the SINRs of UEs as a simple linear function of its respective power allocated [21], enabling to find a matrix of allocated power that obeys the maximum power budget constraint, in simple and expeditious closed-form. We will elucidate how to optimize the passive beamforming at the RIS.

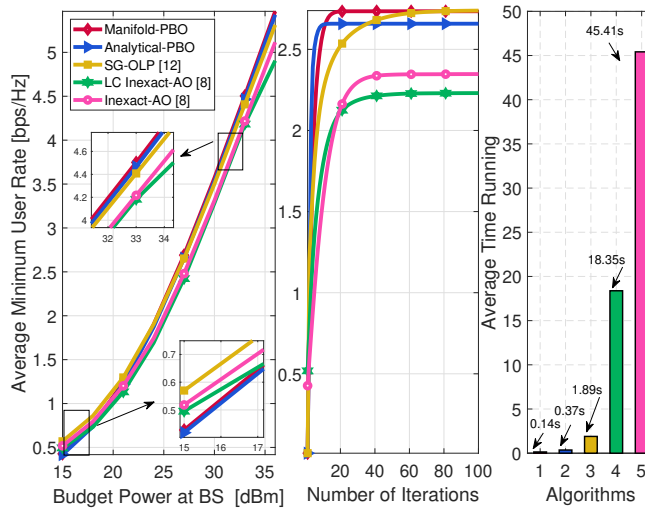




(a) System model of a DL RIS-aided MU mMIMO system.



(b) Steps for the proposed algorithm.



(c) i. Avg.  $\gamma \times P_{\max}$  ii. Avg.  $\gamma \times N_i$  iii. Avg. running time

FIGURE 1: APPLICATION 1: (a) System model of the considered network; (b) Steps of the proposed algorithm; (c) Simulation results.

## Step 2 – Optimizing the Passive Beamforming at the RIS:

- ◊ The major problem is how to maximize the common SINR concerning the reflective passive beamforming. This problem can be formulated as a *minimization of inverse-summation of eigenvalues*, which has an easy and direct way to obtain Euclidean derivative. Therefore, the core of step 2 is to utilize the RCG to optimize the passive reflective beamforming in view to increase as high as possible the common rate shared between all the UEs. Both steps are illustrated in Figure 1b.

Figure 1c compares the performance and complexity of the proposed method for maximizing the minimum rate with the following benchmark schemes:

- ◊ *Inexact-AO* [18]: both the active beamforming and passive reflective beamforming are updated sequentially by AO method. Specifically, active beamforming was solved by CVX as second-order cone programming (SOCP), while the passive beamforming problem was solved deploying SCA. To increase the min-SINR value at each iteration until the convergence, in this approach, only need to find an update for  $\mathbf{W}$  and  $\theta$ .
- ◊ *Low Complexity Inexact-AO* [18]: This method is similar to the Inexact-AO; however, herein, for the passive beamforming, the subgradient projection method is utilized to avoid further complexity.
- ◊ *SG-OLP* [22]: In the sub-gradient (SG)-optimal linear precoder (OLP), the strategy is optimizing the active precoding at BS through the OLP as proposed in [22]. Because of reducing the complexity, the SG method is utilized to optimize the passive beamforming.
- ◊ *Analytical passive beamforming optimization (PBO)*: In this method, we solve exactly the proposed problem, given by Fig. 1b; however, for the **step 2**, we derived a closed-form solution for each element of  $\theta$ , and updated  $\theta_n$  sequentially until the convergence.

Figure 1c.(i) depicts the average common rate  $\bar{\gamma}$  (equivalent to the minimum rate) at UEs versus the maximum transmit power budget  $P_{\max}$ . First, it is observed that the proposed approach considerably outperforms the three benchmark schemes over a wide range of  $P_{\max}$ . This demonstrates the potential of our proposed design, i.e., to optimize the ZF precoding for achieving equal rate conditions and optimize the passive beamforming to maximize the common rate. We also can see that under a lower power regime,  $P_{\max} \leq 19$  dBm, both Inexact-AO, Low-Complexity Inexact-AO, and SG-OLP methods can outperform the proposed method. This is justified because the ZF solution does not operate well for the lower-power regime, differently for the high-power regime, where it is known to be optimal [23].

Figure 1c.(ii) depicts the convergence behavior of our proposed approach, where the maximum transmit power is set as  $P_{\max} = 25$  dBm. It is observed that our RCG

proposed method monotonically increases the common SINR  $\bar{\gamma}$  value over iterations, thus leading to a converged solution. We also can see that all considered algorithms converge in different values. The analytical PBO converges fastest, and the Inexact AO converges slowest. Although the proposed RCG does not achieve the convergence fastest, we can see that it can achieve the best performance, with  $\approx 2.8$  [bps/Hz]. The obtained gains over the Analytical PBO, Inexact-AO, and Low-Complexity Inexact-AO are 3.32%, 19.15%, and 26.13%, respectively. Furthermore, concerning the SG-OLP method, both achieve about the same value in the convergence for the analyzed value of  $P_{\max}$ , proofing the potential of the proposed solution since the running time for the manifold approach is substantially lower, as we discuss in the following.

Figure 1c.(iii) illustrates the average running time of each algorithm considered. From this figure, we can see how it is important to consider the **step 1** of the proposed algorithm since this step is crucial for time reduction, providing low-running time over the Inexact-AO and Low Complexity Inexact-AO algorithms. This is expected, as **step 1** eliminates the AO methodology from the algorithm, remarkably reducing its complexity. The high time running for Inexact-AO is attributed to the repeated solving of two different convex problems until convergence, which is time-consuming due to its dependence on CVX. On the other hand, the Low-Complexity Inexact-AO can reduce the complexity since instead of two convex problems, it solves just one convex problem (active beamforming at BS), while the subgradient method is utilized for passive beamforming. Concerning the SG-OLP method, our proposed approach still can be further promising in terms of complexity since the OLP method requires solving a fixed point equation followed by the SG method, iteratively, up to the convergence. On the other hand, for this problem, our proposed method does not require any iterative process over the active and passive beamforming.

### B. Application 2: RIS-Aided Energy-Efficient mMIMO for IoT Systems

The need for efficient wireless communication is more critical than ever, especially with the rise of IoT applications. Optimizing UL power allocation is essential for enhancing communication performance. By leveraging advanced technologies such as RIS combined with the linear minimum mean squared error (MMSE) receiver, significant improvements can be achieved in how IoT devices communicate with BSs. To do this efficiently, instantaneous CSI is crucial for optimizing communication. By knowing the CSI, the BS can effectively allocate UL power and control the RIS phase shifts. This information allows the BS to send specific power indicators and phase shift vectors to IoT devices, enhancing their communication with the BS. This application is about how to get the most energy-efficient mMIMO systems working with RIS. One can use optimization tools based on MO

methods and procedures, confirming the suitable outcomes achieved using MO approach.

To tackle the non-convexity of the problem, an RM-based iterative-alternating optimization (i-AO) technique was deployed. The RM i-AO algorithm makes the system much more efficient in terms of EE and resource-efficient (SE-EE tradeoff) than the non-EE MU mMIMO system. EE RM-based optimization methodology for RIS-aided mMIMO includes formulate and solve the optimization problem using RM-based i-AO algorithm:

- ◇ Formulate the EE power minimization problem in the UL RIS-aided mMIMO IoT network and establish a solution methodology based on the RM approach.
- ◇ Develop an optimization methodology for EE power minimization problem in different RIS-aided mMIMO system configurations by deploying specific MO formulations and tools.
- ◇ KPI, including: a) SE  $\times$  EE tradeoff maximization; b) precoding/combining design; c) effective power allocation strategies for mMIMO.

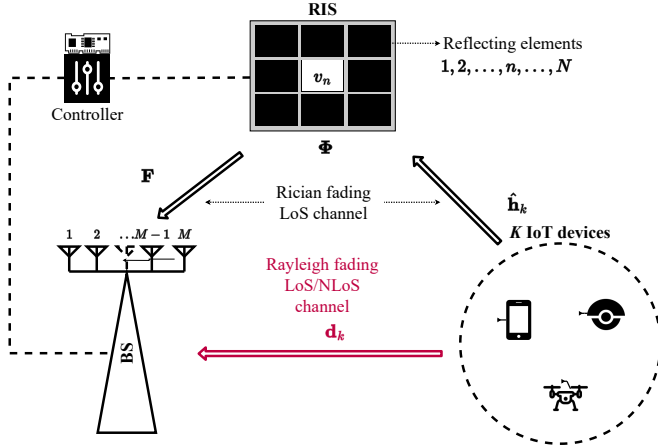
We deploy an RM-based AO technique for optimizing the RIS phase shifts and the BS receiver-combiner vectors. In the context of an IoT network with RIS support, this technique aims to reduce the UL transmit power of the UEs. Initially, the joint optimization for the RIS phase shift and BS combining vectors is formulated to improve the overall system EE by minimizing the UL transmit power while guaranteeing a minimum QoS for the devices.

**System Model:** Consider the UL of multiple access mMIMO systems, where  $K$  IoT single-antenna devices transmit simultaneously to a BS equipped with  $M$  antennas, representing a typical mMIMO scenario (Figure 2a). Strategically positioning a RIS can substantially improve system reliability, facilitating communication between users and the BS. The RIS contains  $N$  reconfigurable reflecting elements. The RIS delivers a phase-shifted version of the transmitted signal, maximizing the composite channel gain. Moreover, the DL dual problem can be considered similarly, being omitted herein.

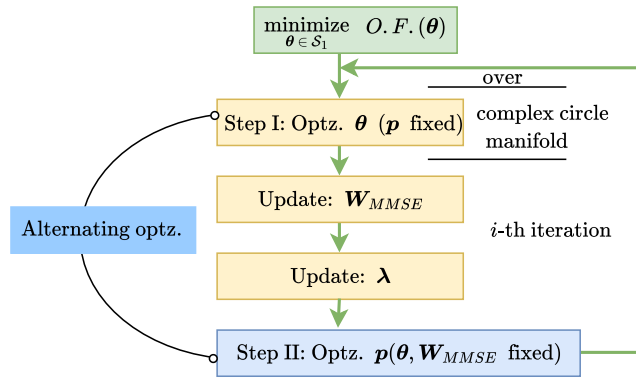
The signal's power is carefully controlled when each IoT device transmits data. The data signal of an IoT device combines its transmit power and a normalized data symbol. This setup ensures that each device can communicate effectively while minimizing interference with other devices.

**Problem Formulation:** to minimize the UL power while maintaining high SE<sup>4</sup>, we need to optimize the RIS phase shift vector ( $\theta$ ), the BS beamforming matrix ( $W$ ), and

<sup>4</sup>The metric SE measures how effectively the available bandwidth is utilized. The SE of an IoT device depends on its transmit power, the combining vector at the BS, and the channel conditions. By optimizing these factors, one is doing SE maximization, ensuring that each device transmits data efficiently.



(a) Illustration of a passive RIS-aided MU mMIMO system.



(b) i-AO steps for the proposed algorithm attain convergence.

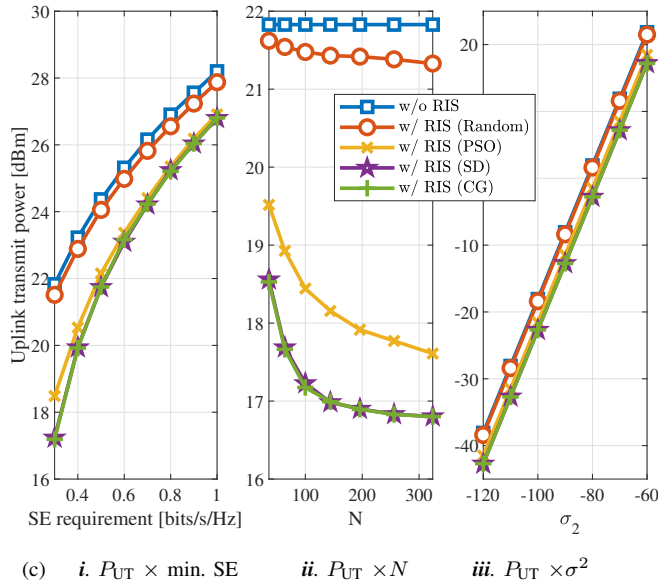


FIGURE 2: APPLICATION 2: (a) System model for the considered network; (b) Steps of the proposed algorithm; (c) UL transmit power ( $P_{UT}$ ) with  $K = 8$  varying: *i*) min SE; *ii*) number of reflective elements  $N$ ; *iii*) noise power at BS.

the power vector of the devices ( $\mathbf{p}$ ). This involves several constraints:

- Ensuring each device meets its QoS requirements.
- Maintaining the unit-modulus of the RIS phase shift.
- Keeping the BS combining matrix normalized.
- Ensuring the device power stays within maximum limits ( $P_{\max,k}$ ).

**Proposed Solution:** an effective approach to solving this optimization problem is the AO. This method involves iterative and sequentially optimizing different variables while keeping others fixed. Herein, we adopt an i-AO based on a CCM, which alternately solves the power allocation (EE optimization), beamforming, and RIS phase shift optimization variables for a generic RIS-aided mMIMO system as illustrated in Figure 2b. The i-AO optimization steps were implemented as follows:

**Step 1 – Fix Power Allocation:**

- ◇ Initially, the power allocation for IoT devices is fixed. Using the linear MMSE receiver ( $\mathbf{W}_{MMSE}$ ), the BS combining vectors are determined.

**Step 2 – Optimize RIS Phase Shifts ( $\theta$ ):**

- ◇ The RIS phase shifts are then optimized using a manifold-based approach, which respects the complex constraints of the phase shifts.

**Step 3 – Update BS Combining Matrix ( $\mathbf{W}_{MMSE}$ ):**

- ◇ After optimizing the phase shifts, the BS combining matrix is updated accordingly.

**Step 4 – Update the Lagrangian multipliers ( $\lambda$ ):**

- ◇ Since we apply the Lagrangian relaxation to move the complicated SE requirement constraint to the OF, it is necessary to update the Lagrangian multipliers.

**Step 5 – Adjust Device Power ( $\mathbf{p}$ ):**

- ◇ Finally, the power allocation is optimized, ensuring that each device operates within its power limits while meeting SE requirements.

Comparative results for UL transmit power as a function of min-SNR, number of reflective elements, and noise power at BS are illustrated in Figure 2c, where PSO represents the PSO-based manifold scheme; SD: steepest-descent for RM, and CG holds for the classical conjugate gradient manifolds. Unless stated otherwise, we assume  $K = 8$  users are positioned evenly along a semicircle with a radius of 20 meters centered on a RIS. The distance from the RIS to the BS is 700 meters. Using such a scenario, the distance between users and the BS is derived geometrically. The path loss factors between the links are:  $\alpha_k$  (UTs-RIS) = 2,  $\beta$  (BS-RIS) = 2.5, and  $\gamma_k$  (BS-UTs) = 4. Additionally, we use  $M = 64$ ,  $N = 100$ ,  $P_{\max,k} = 30$  dBm, and  $\sigma^2 = -104$  dBm. The line-of-sight (LoS) channel angles are

randomly generated between 0 and  $2\pi$ . MCs are conducted by calculating averages over  $10^4$  realizations.

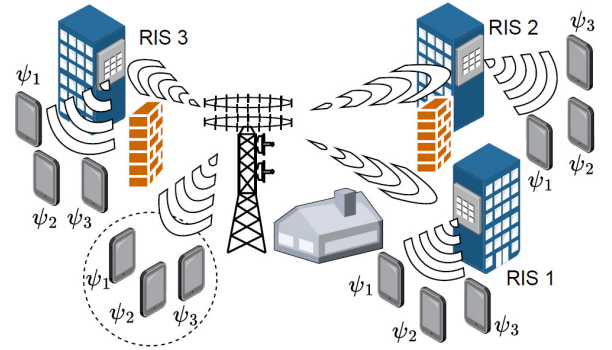
In Figure 2c, three scenarios are considered, using the total UL transmission power as the metric. In all cases, it is observed that systems without RIS and systems with RIS but without optimized reflection phases exhibit the worst conditions, requiring higher  $P_{UT}$  to meet the minimum requirements for all users. Furthermore, in all the considered scenarios, the SD and CG manifold schemes demonstrated nearly identical performance. Notably, without phase shift optimization for the RIS elements, the performance gain from employing the RIS is not substantial. Conversely, with both the SD and CG schemes, there is a reduction in  $P_{UT}$  of approximately 50 to 60%, depending on target values of SE, number RIS elements and noise power. Even the PSO-based manifold scheme achieves a power saving of around 40 to 50%, which is significant given its considerably lower complexity compared to the other optimization schemes.

### C. Application 3: RIS-Enabled Intra-Cell Pilot Reuse

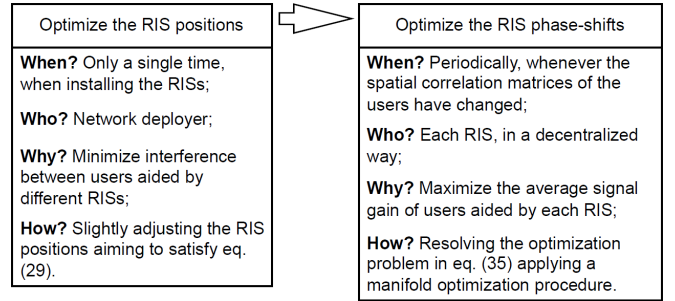
Since the inception of mMIMO technology, pilot contamination has been the main bottleneck of such systems. The impossibility of allocating orthogonal pilot sequences for every user in the system due to the limited channel coherence blocks leads to the necessity of reusing pilots, which thus results in a directed interference known as pilot contamination. Therefore, a crucial trade-off arises in the system design between the number of orthogonal pilots and the associated overhead for their UL transmission, which can severely penalize the system's SE. As more pilots are reused, the channel estimation overhead improves spectral efficiencies if the associated pilot contamination remains under control.

Given the above scenario, another quite appealing use case for RISs is *enabling intra-cell pilot reuse* in a mMIMO system. Authors in [24] have shown that, given a set of orthogonal pilots already in use in a cell, each additional RIS employed at the cell enables the total reuse of such pilot set among the users aided by that RIS. This is equivalent to having  $\tau_p$  orthogonal pilots in a cell with  $R$  RISs, up to  $K = (R + 1)\tau_p$  users can be served. This scenario is illustrated in Figure 3a.

A two-stage methodology is proposed to make it possible while controlling the intra-cell pilot contamination. The first stage consists of optimizing the deployment locations of the RISs, with an angular grid being obtained as the optimized positions, leading to reduced interference between the users served by different RISs. The second stage consists of optimizing the RIS phase shifts to maximize the average channel gain of the RIS-aided users, which is done by applying the MO framework based solely on the statistical CSI of the users. This latter feature has the advantage of requiring less frequent RIS re-configurations, simplifying channel estimation since the isolated BS-RIS and RIS-UEs channels are not needed, reducing the necessity of deploying

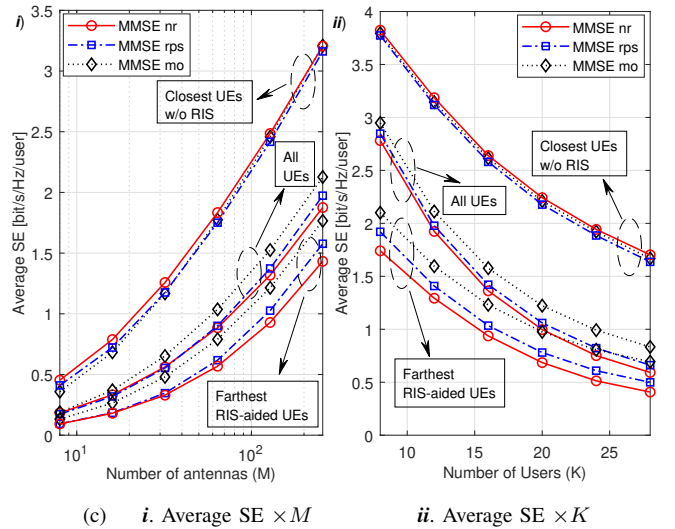


(a) MU mMIMO assisted by multiple RISs.



(b) Stage 1

Stage 2.



(c) i. Average SE  $\times M$

ii. Average SE  $\times K$

FIGURE 3: APPLICATION 3:(a) MU mMIMO communication system assisted by multiple RISs, each deployed on the facades of buildings. The users in the dotted circle area are served without the aid of any RIS. They, as well as the users served by each RIS, share the same set of pilot sequences in our investigated scenario. (b) Execution tasks of the **two stages RIS-aided pilot reuse method**; (c) UL SE with  $N = 256$ ,  $\tau_p = 4$ , and increasing: i.  $M$ , when  $R = 3$ , and  $K = 16$  UEs; ii.  $K$ ,  $R$ , and  $\varsigma$ , such that  $K = \varsigma \tau_p = (R + 1) \tau_p$ , when  $M = 128$  antennas at the BS.



active elements at the RIS side. Figure 3b summarizes the main characteristics of each stage.

Figure 3c.(i) depicts the average SE performance with the increasing number of BS antennas, considering  $R = 3$ ,  $N = 256$ , and  $K = 16$  UEs sharing  $\tau_p = 4$  pilots. It shows the average performances taking into account only the closest UEs not aided by any RIS, only the farthest RIS-aided UEs, and all UEs as well. It employs the MMSE detector while considering as benchmarks the mMIMO system without RIS (denoted as  $nr$ ), and a scheme employing RIS with random phase shifts (denoted as  $rps$ ). On the other hand, the results with the RIS employing phase shifts obtained via the MO approach are denoted by  $mo$ . One can see that the SE performance of the closest UEs does not suffer significant changes employing the proposed approach, while the average SE per user performance of the farthest UEs is improved regarding  $nr$  and  $rps$  approaches. This occurs since the average channel gain of the RIS-aided UEs increases, and the resultant effect is an improvement in the SE when averaged between all UEs. The farthest UEs' SE employing  $M = 128$  antennas increases from 0.929 bit/s/Hz without RIS to 1.026 bit/s/Hz ( $\approx 10\%$ ) with  $rps$  and 1.214 bit/s/Hz ( $\approx 31\%$  gain in SE) with  $mo$  method. When averaging between all UEs, the performance also increases  $\approx 16\%$  with  $mo$  in comparison with no RIS scheme.

Then, it is kept fixed the number of pilots as  $\tau_p = 4$  and the number of BS antennas as  $M = 128$ , while the pilot-reuse factor (PRF)  $\zeta$  increases together with the number of RISs and UEs, such that  $\zeta = R + 1 = K/\tau_p$  holds. Figure 3c.(ii) depicts how the UL SE is affected by such aggressive intra-cell pilot-reuse scenarios while showing that the proposed methodology effectively leverages the RISs to improve performance in these challenging conditions. One can see an almost linear increase of  $\approx 0.3$  bit/s/Hz per UE achieved with  $mo$  compared with no RIS strategy when averaging between the farthest RIS-aided UEs. As such UEs are a fraction of  $\frac{\zeta-1}{\zeta}$  of the total number of UEs; the UL SE gain when averaging between all UEs starts from  $\approx 0.16$  bit/s/Hz and gradually converges to the same increase of  $\approx 0.3$  bit/s/Hz as  $K$  increases. Besides, if one fixes a target UL SE performance of 1 bit/s/Hz, the number of UEs can be increased from 20 to 24 when employing the proposed methodology, with neither an increase in the training overhead nor significant increases in power consumption or processing complexity.

#### D. Application 4: RIS-Aided Grant-Free Random Access for Massive Machine-Type Communication (mMTC)

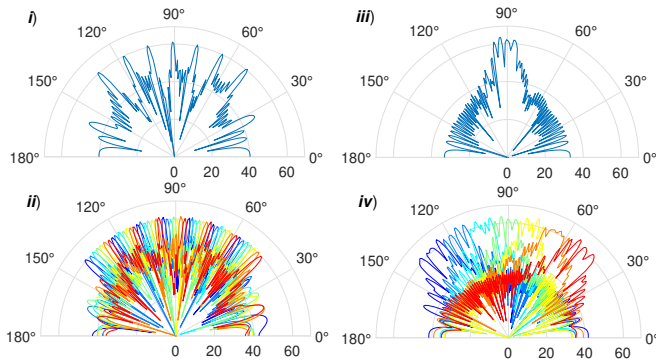
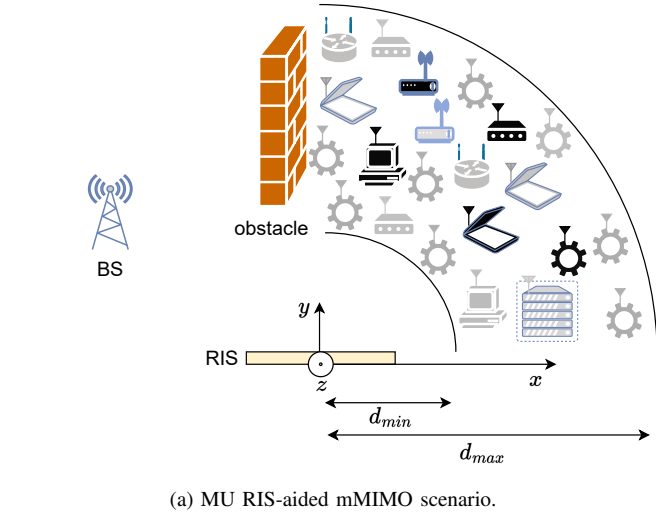
Empowered by the rapid development of IoT applications, the mMTC scenario will play an essential role in the upcoming 6G technology. The enormous number of machine type communications (MTC) devices usually have sparse activities and low data volumes to transmit, thus requiring new access technologies, which should be decentralized and uncoordinated for scalability. RISs can be leveraged to

improve the connectivity of the mMTC network, improving the channel propagation conditions while simultaneously managing access to the communication channels, (Figure 4a). GF RA is a suitable solution for such scenarios, aiming to avoid the excessive overhead of acquiring a grant and performing centralized scheduling procedures. Therefore, another appealing use case for the RISs involves developing RIS-aided GF RA protocols for mMTC systems.

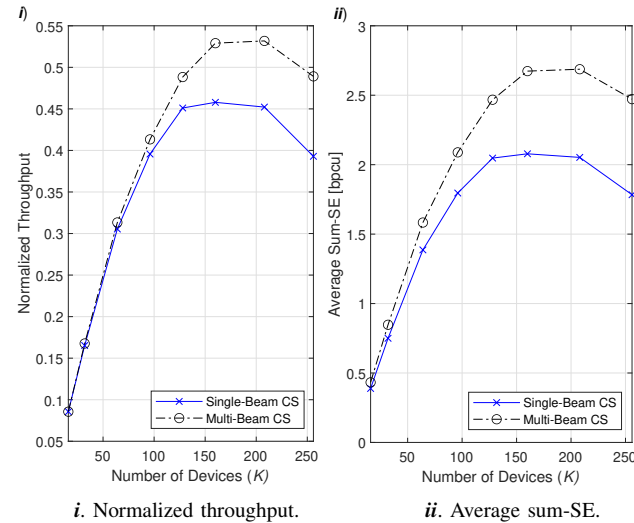
**GF-RA protocol under single-beam RIS passive beamforming:** A scheme is proposed in [25], which consists of a 2-step protocol. In the first step, the BS transmits DL pilot signals while the RIS sweeps its reflection configuration to cover all the devices' areas. The devices receive these reflected pilots and can thus learn which RIS configuration leads to the highest channel gain for them in the so-called channel sounding (CS) procedure. In the second stage, the RIS again sweeps its reflection configurations while the devices transmit their payloads in the time slot corresponding to their chosen RIS configuration from the previous step. Since the devices are supposed to be uniformly distributed in the covered area, their access in the protocol's second step tends to be uniformly distributed, minimizing collisions and improving channel gains simultaneously.

**GF-RA protocol under multi-beam RIS passive beamforming (PBF):** The single-beam approach can lead to a significant training overhead since many communication resources are usually required in the first step to exhaustively sweep the RIS configuration among the whole covered area with a single beam per time. To overcome this limitation, a promising solution is to replace the single-beam training approach with a multi-beam one, which should cover the whole devices' area and allow them to find their best RIS reflection configuration in a reduced training interval. For this sake, the multi-beam RIS configurations can be designed in two stages: the first one is composed of consecutive beams, which allows the devices to discover to which sector of the covered region they belong; the second one is composed of interleaved beams, and allows the devices to discover in which portion of the sector they are located. However, for the multi-beam reflection design, a simple linear combination of DFT steering vectors does not satisfy the unit modulus constraint and is not easily generated in a passive RIS. Therefore, an optimization problem can be formulated to obtain a uniform high-gain reflected multi-beam in the intended directions while keeping low reflection gains in the unintended ones, subject to the unit modulus constraint. Once again, the MO framework shows to be a promising tool to solve such optimization problems, as discussed in [26], and can be adapted to design the RIS-aided GF-RA protocol. Figure 4b depicts the multi-beam reflection patterns obtained by the MO framework.

Figure 4c evaluates the performance of the RIS-aided GF-RA protocols employing single-beam and multi-beam channel sounding approaches. It first compares the normal-



(b) *i*) Single interleaved multi-beam reflection pattern; *ii*) temporal sequence of interleaved multi-beams covering  $[45^\circ; 135^\circ]$ ; *iii*) a single consecutive multi-beam reflection pattern; *iv*) temporal sequence of consecutive multi-beams covering  $[45^\circ; 135^\circ]$



(c) RA performance of the RIS-aided GF protocol with multi-beam channel.

FIGURE 4: APPLICATION 4: (a) System model; (b) multi-beam reflection patterns designed via MO; (c) RA performance of the GF protocol.

ized throughput performance, defined as the ratio between the number of succeeding devices and available resources. The investigated scenario is composed of a mMIMO BS with 128 antennas aided by a RIS with  $64 \times 4$  elements in the horizontal and vertical dimensions, respectively. For simplicity, both BS, RIS, and devices are assumed to be in the same horizontal plane; therefore, up to 64 DFT-based orthogonal beams could be used, among which only 46 falls in the considered devices region between  $45^\circ$  and  $135^\circ$ , which are those employed in the access stage (step 2). In each access stage, the devices also transmit a random pilot sequence of length  $\tau_p = 4$ , which may allow them to successfully access the same beam provided they choose different pilots and achieve an SINR above the decoding threshold. Thus, the normalized throughput in this scenario is the number of succeeding devices divided by 184, which is the total number of resources combining beams and pilots in the access stage. As can be seen from Figure 4c.(i), the multi-beam CS approach achieves a maximum normalized throughput of 0.5318, which, compared to 0.4579 achieved by the single-beam one, represents a remarkable improvement of 16.14%. On the other hand, Figure 4c.(ii) evaluates the sum-SE of the network, which also accounts for the lower overhead required by the multi-beam CS approach. While the single-beam CS approach needs 46-time slots in step 1 in the evaluated scenario, the multi-beam approach can evaluate step 1 with only 14-time slots. This is accomplished by expanding the targeted area in 49 beams, scanned in 7 configurations of 7 consecutive multi-beams, followed by another 7 configurations of 7 interleaved multi-beams, as depicted in Figure 4b. In this way, the multi-beam CS approach achieves a maximum sum-SE of 2.6873 bpcu, which, in comparison with 2.0783 bpcu achieved by the single-beam one, represents an important improvement of 29.3%. Besides, it is worth mentioning that there is room for larger gains if the reflection patterns are further improved (reducing side-lobe levels and beam ripple), and/or if the multi-beam reflection approach is also leveraged in the access stage.

## VII. CONCLUSION

MO provides a structured and powerful approach to tackling complex optimization problems in wireless communication systems, especially in RIS-aided mMIMO systems scenarios for next-generation wireless communications, offering significant advantages over conventional optimization methods. By leveraging the geometric properties of the manifold, we can achieve more efficient and effective solutions compared to conventional optimization methods. MO methods offer significant advantages over traditional optimization methods in wireless communications, particularly in handling non-convex constraints and high-dimensional data. While heuristic evolutionary algorithms, convex relaxation techniques, and gradient-based methods each have their merits, MO methods provide a more natural and efficient framework for solving complex optimization problems in this domain.

The key advantages of MO methods include their ability to exploit geometric properties, manage high-dimensional data, and handle various constraints and symmetries, making them particularly well-suited for next-generation wireless communication systems.

We have explored in details five applications of the MO framework aiming to optimizing RIS-aided mMIMO wireless communication systems; we have proposed: a) an efficient MO-based algorithm for optimizing the beamforming weights and RIS phase shifts, maximizing the sum of received SINRs; b) maximize the minimum rate of the network by leveraging RCG within a CCM; c) an RM-based RIS phase shift optimization method aimed at minimizing the UL transmit power in IoT networks with RIS; d) RIS phase shifts optimization method for intra-cell pilot reuse with statistical CSI using MO methodology, highlighting remarkable performance improvements in both UL and DL transmissions; e) multi-beam design optimization problem in a RIS-based GF random access protocol. A key advantage of the MO approach is the ability to handle non-convex constraints naturally. These applications illustrate the substantial benefits of using MO techniques to enhance the performance, fairness, and efficiency of RIS-aided mMIMO systems.

## REFERENCES

- [1] J. Wu, S. Kim, and B. Shim, "Energy-Efficient Power Control and Beamforming for Reconfigurable Intelligent Surface-Aided Uplink IoT Networks," *IEEE Transactions on Wireless Communications*, vol. 21, DOI 10.1109/TWC.2022.3182773, no. 12, pp. 10 162–10 176, 2022.
- [2] E. Shtaiwi, H. Zhang, A. Abdelhadi, A. L. Swindlehurst, Z. Han, and H. V. Poor, "Sum-Rate Maximization for RIS-Assisted Integrated Sensing and Communication Systems With Manifold Optimization," *IEEE Transactions on Communications*, vol. 71, DOI 10.1109/TCOMM.2023.3277872, no. 8, pp. 4909–4923, 2023.
- [3] R. Liu, M. Li, Q. Liu, and A. L. Swindlehurst, "Joint Symbol-Level Precoding and Reflecting Designs for IRS-Enhanced MU-MISO Systems," *IEEE Transactions on Wireless Communications*, vol. 20, DOI 10.1109/TWC.2020.3028371, no. 2, pp. 798–811, 2021.
- [4] X. Yu, D. Xu, and R. Schober, "Optimal Beamforming for MISO Communications via Intelligent Reflecting Surfaces," in *2020 IEEE 21st International Workshop on Signal Processing Advances in Wireless Communications (SPAWC)*, DOI 10.1109/SPAWC48557.2020.9154337, pp. 1–5, 2020.
- [5] M. A. ElMossallamy, K. G. Seddik, W. Chen, L. Wang, G. Y. Li, and Z. Han, "RIS Optimization on the Complex Circle Manifold for Interference Mitigation in Interference Channels," *IEEE Transactions on Vehicular Technology*, vol. 70, DOI 10.1109/TVT.2021.3073158, no. 6, pp. 6184–6189, 2021.
- [6] H. Guo, Y.-C. Liang, J. Chen, and E. G. Larsson, "Weighted Sum-Rate Maximization for Intelligent Reflecting Surface Enhanced Wireless Networks," in *2019 IEEE Global Communications Conference (GLOBECOM)*, DOI 10.1109/GLOBECOM38437.2019.9013288, pp. 1–6, 2019.
- [7] T. Jiang and W. Yu, "Interference Nulling Using Reconfigurable Intelligent Surface," *IEEE Journal on Selected Areas in Communications*, vol. 40, DOI 10.1109/JSAC.2022.3143220, no. 5, pp. 1392–1406, 2022.
- [8] J. V. Alegría and F. Rusek, "Channel Orthogonalization with Reconfigurable Surfaces," in *2022 IEEE Globecom Workshops (GC Wkshps)*, DOI 10.1109/GCWkshps56602.2022.10008751, pp. 37–42, 2022.
- [9] Y. Xiu, J. Zhao, W. Sun, M. D. Renzo, G. Gui, Z. Zhang, and N. Wei, "Reconfigurable Intelligent Surfaces Aided mmWave NOMA: Joint Power Allocation, Phase Shifts, and Hybrid Beamforming Optimization," *IEEE Transactions on Wireless Communications*, vol. 20, DOI 10.1109/TWC.2021.3092597, no. 12, pp. 8393–8409, 2021.
- [10] B. Xu, J. Zhang, H. Du, Z. Wang, Y. Liu, D. Niyato, B. Ai, and K. B. Letaief, "Resource Allocation for Near-Field Communications: Fundamentals, Tools, and Outlooks," *IEEE Wireless Communications*, DOI 10.1109/MWC.016.2300528, pp. 1–9, 2024.
- [11] X. Li, Z. Xie, Z. Chu, V. G. Menon, S. Mumtaz, and J. Zhang, "Exploiting Benefits of IRS in Wireless Powered NOMA Networks," *IEEE Transactions on Green Communications and Networking*, vol. 6, DOI 10.1109/TGCN.2022.3144744, no. 1, pp. 175–186, 2022.
- [12] M. AlaaEldin, E. Alsusa, K. G. Seddik, M. Al-Jarrah, and C. Papadias, "Optimization of Energy-Constrained IRS-NOMA Using a Complex Circle Manifold Approach," *IEEE Internet of Things Journal*, DOI 10.1109/IJOT.2024.3427425, pp. 1–1, 2024.
- [13] N. Boumal, B. Mishra, P.-A. Absil, and R. Sepulchre, "Manopt, a Matlab Toolbox for Optimization on Manifolds," *Journal of Machine Learning Research*, vol. 15, no. 42, pp. 1455–1459, 2014. [Online]. Available: <https://www.manopt.org>
- [14] N. Boumal, *An introduction to optimization on smooth manifolds*, 1st ed. UK: Cambridge University Press, Sep. 2023, <https://cambridge.org/9781009166157>.
- [15] P.-A. Absil, R. Mahony, and R. Sepulchre, *Optimization Algorithms on Matrix Manifolds*. USA: Princeton University Press, 2007.
- [16] J. Hu, X. Liu, Z.-W. Wen, and Y.-x. Yuan, "A Brief Introduction to Manifold Optimization," *Journal of the Operations Research Society of China*, vol. 8, DOI 10.1007/s40305-020-00295-9, 04 2020.
- [17] M. Meilä and H. Zhang, "Manifold learning: What, how, and why," *Annual Review of Statistics and Its Application*, vol. 11, DOI <https://doi.org/10.1146/annurev-statistics-040522-115238>, no. Volume 11, 2024, pp. 393–417, 2024. [Online]. Available: <https://www.annualreviews.org/content/journals/10.1146/annurev-statistics-040522-115238>
- [18] H. Xie, J. Xu, and Y.-F. Liu, "Max-Min Fairness in IRS-Aided Multi-Cell MISO Systems With Joint Transmit and Reflective Beamforming," *IEEE Transactions on Wireless Communications*, vol. 20, DOI 10.1109/TWC.2020.3033332, no. 2, pp. 1379–1393, 2021.
- [19] H. Yu, H. D. Tuan, A. A. Nasir, T. Q. Duong, and H. V. Poor, "Joint Design of Reconfigurable Intelligent Surfaces and Transmit Beamforming Under Proper and Improper Gaussian Signaling," *IEEE Journal on Selected Areas in Communications*, vol. 38, DOI 10.1109/JSAC.2020.3007059, no. 11, pp. 2589–2603, 2020.
- [20] Q.-U.-A. Nadeem, H. Alwazani, A. Kammoun, A. Chaaban, M. Debbah, and M.-S. Alouini, "Intelligent Reflecting Surface-Assisted Multi-User MISO Communication: Channel Estimation and Beamforming Design," *IEEE Open Journal of the Communications Society*, vol. 1, DOI 10.1109/OJCOMS.2020.2992791, pp. 661–680, 2020.
- [21] H. Zhang, B. Di, Z. Han, H. V. Poor, and L. Song, "Reconfigurable Intelligent Surface Assisted Multi-User Communications: How Many Reflective Elements Do We Need?" *IEEE Wireless Communications Letters*, vol. 10, DOI 10.1109/LWC.2021.3058637, no. 5, pp. 1098–1102, 2021.
- [22] A. Papazafeiropoulos, P. Kourtessis, and S. Chatzinotas, "Max-Min SINR Analysis of STAR-RIS Assisted Massive MIMO Systems With Hardware Impairments," *IEEE Transactions on Wireless Communications*, vol. 23, DOI 10.1109/TWC.2023.3316707, no. 5, pp. 4255–4268, 2024.
- [23] C. Huang, A. Zappone, G. C. Alexandropoulos, M. Debbah, and C. Yu, "Reconfigurable Intelligent Surfaces for Energy Efficiency in Wireless Communication," *IEEE Transactions on Wireless Communications*, vol. 18, DOI 10.1109/TWC.2019.2922609, no. 8, pp. 4157–4170, 2019.
- [24] J. C. Marinello, T. Abrão, E. Hossain, and A. Mezghani, "Reconfigurable Intelligent Surfaces-Enabled Intra-Cell Pilot Reuse in Massive MIMO Systems," *IEEE Transactions on Wireless Communications*, DOI 10.1109/TWC.2024.3362517, pp. 1–1, 2024.
- [25] V. Croisfelt, F. Saggese, I. Leyva-Mayorga, R. Kotaba, G. Gradoni, and P. Popovski, "Random Access Protocol With Channel Oracle Enabled by a Reconfigurable Intelligent Surface," *IEEE Transactions on Wireless Communications*, vol. 22, DOI 10.1109/TWC.2023.3268765, no. 12, pp. 9157–9171, 2023.
- [26] P. Wang, J. Fang, L. Dai, and H. Li, "Joint Transceiver and Large Intelligent Surface Design for Massive MIMO mmWave Systems," *IEEE Transactions on Wireless Communications*, vol. 20, DOI 10.1109/TWC.2020.3030570, no. 2, pp. 1052–1064, 2021.